

# Efficient Deep Demosaicing with Spatially Downsampled Isotropic Networks

Cory Fan\*  
 Cornell University  
 Ithaca, NY 14853, USA  
 cyf5@cornell.edu

Wenchao Zhang  
 OmniVision Technologies  
 Santa Clara, CA 95054, USA  
 wenchao.zhang@ovt.com

## Abstract

In digital imaging, image demosaicing is a crucial first step which recovers the RGB information from a color filter array (CFA). Oftentimes, deep learning is utilized to perform image demosaicing. Given that most modern digital imaging applications occur on mobile platforms, applying deep learning to demosaicing requires lightweight and efficient networks. Isotropic networks, also known as residual-in-residual networks, have been often employed for image demosaicing and joint-demosaicing-and-denoising (JDD). Most demosaicing isotropic networks avoid spatial downsampling entirely, and thus are often prohibitively expensive computationally for mobile applications. Contrary to previous isotropic network designs, this paper claims that spatial downsampling to a significant degree can improve the efficiency and performance of isotropic networks. To validate this claim, we design simple fully convolutional networks with and without downsampling using a mathematical architecture design technique adapted from DeepMAD, and find that downsampling improves empirical performance. Additionally, empirical testing of the downsampled variant, JD3Net, of our fully convolutional networks reveals strong empirical performance on a variety of image demosaicing and JDD tasks.

## 1. Introduction

Demosaicing is a first and crucial step in an Image Sensor Processing (ISP) pipeline [7]. Recent advances in mobile photography, including more challenging non-Bayer CFA mosaics and pixel binning techniques, have made the task of demosaicing in modern mobile phones increasingly difficult [28]. Thus, deep learning techniques for non-Bayer demosaicing have been increasingly explored [23, 24, 28]. However, deep learning techniques are infamously compute-heavy, which poses challenges for usage on a mobile plat-

\*Work completed principally when Cory Fan was an intern at Omnivision.

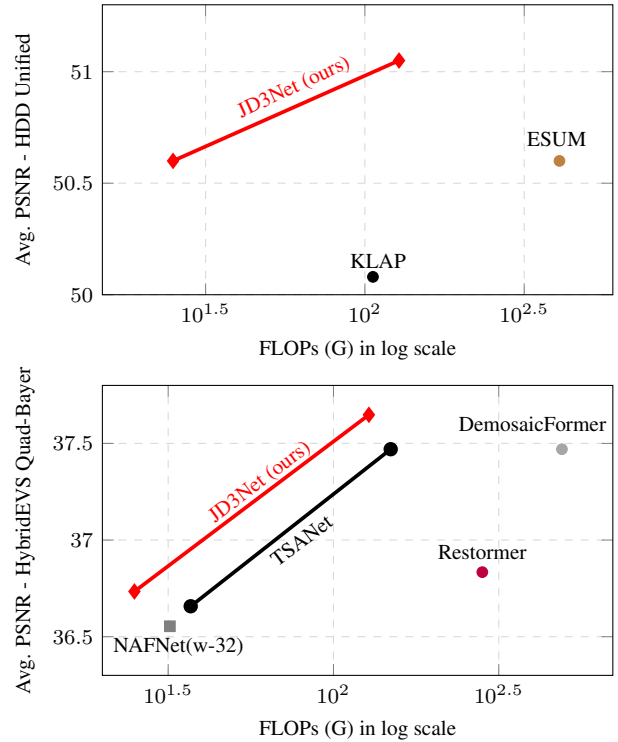


Figure 1. PSNR vs. computational cost on unified joint-demosaicing-and-denoising on HDD (top) and Quad-Bayer HybridEVS demosaicing (bottom).

form. Consequently, lightweight networks are essential for demosaicing on mobile phones [38].

One major class of image demosaicing network are isotropic networks, which are often called residual-in-residual networks [15, 28, 30]. These networks are characterized by their entire trunk maintaining the same spatial resolution; one particularly well-known example is the Vision Transformer (ViT) architecture[4]. However, unlike ViT networks, which perform aggressive patch-ification to reduce computational cost, isotropic networks for demosaicing largely perform their computations on the full spa-

tial resolution of the image (or nearly so), consequently leading to a comparatively higher computational cost. This particular property of isotropic image demosaicing networks seems to be inherited from the strong success of isotropic networks in super-resolution[2, 13, 35]. On the contrary, for the task of image demosaicing, we find that spatial downsampling is effective for improving performance and efficiency in FLOP-equivalent network variants.

Reasoning about the effect of singular variables in designing deep networks can often be challenging, due to the dozens of interdependent hyperparameters found in network architectures. We employ two measures to enable empirical testing of the effects of downsampling. First, we consider only very simple fully-convolutional isotropic networks, which reduces our search space to only three variables: depth, width, and downsampling factor. Next, to produce principled and fair candidate variants of downsampled and non-downsampled networks, we employ a mathematical architecture design technique modified from DeepMAD[25]. Our results show that downsampling improves the performance of two FLOP-equivalent networks, especially in particularly small networks.

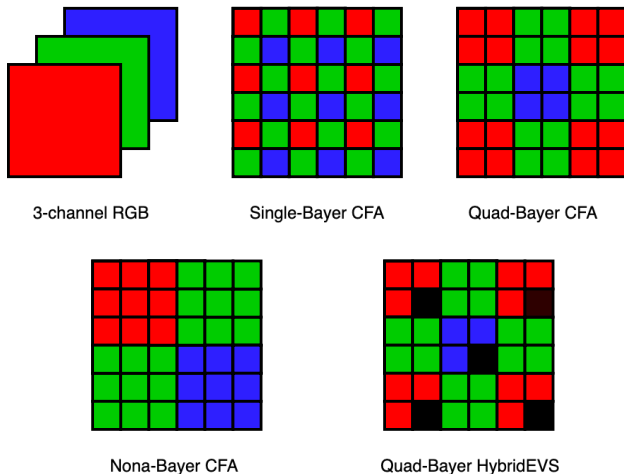


Figure 2. CFAs investigated in this paper. Networks often have to deal with challenging CFAs with missing information (HybridEVS CFA, for instance) or multiple CFA simultaneously.

Recent work in image demosaicing has explored complex patterns[23, 24, 38] and techniques to create unified models[11, 28]. Following this diversity in recent image demosaicing work, we test the applicability of downsampled networks to a variety of tasks. Our downsampled networks, which we term JD3Net (**J**oint **D**emosaicing and **D**enoising with **D**ownsampled **N**etwork), are highly simple fully convolutional networks, but nonetheless we find that they achieve state-of-the-art efficiency on unified Bayer/non-Bayer joint-demosaicing-and-denoising, classical Bayer image demosaicing, and quad-Bayer HybridEVS

image demosaicing (see Fig. 1). An overview of the CFA patterns considered can be found in Fig. 2. Overall, we argue that downsampling can broadly improve the efficiency of deep networks across a variety of image demosaicing tasks.

## 2. Related Work

### 2.1. Tasks in Demosaicing

Modern methods for classical Bayer demosaicing, including deep learning methods, can reconstruct RGB images with a high-degree of precision. Nonetheless, numerous challenges still exist in the field of demosaicing, including joint-demosaicing-and-denoising and non-Bayer demosaicing techniques.

Joint demosaicing and denoising (JDD) is a deep learning task that combines two image processing steps – demosaicing and denoising – into one end-to-end objective. JDD is attractive because it preserves the decorrelated noise of raw images while maintaining the full information of the raw image for demosaicing[5]; consequently, research in this direction has existed even before the popularization of deep learning [9]. Nonetheless, deep learning approaches have been the mainstream in JDD research recently. Typically, a convolutional neural network (CNN) variant is applied to this task [15, 23, 24, 28, 30], with some exceptions [31, 38].

While early JDD research was largely based on the traditional Bayer CFA [15, 20, 30], modern research often focuses on non-Bayer demosaicing[23, 24, 37, 38] or unified Bayer/non-Bayer demosaicing[11, 28]. Non-Bayer CFAs tend to be more challenging, and can even have pixels with completely zero information, such as in HybridEVS image demosaicing. The difficulty of non-Bayer demosaicing, even without the denoising task, similarly merits deep learning.

### 2.2. Isotropic Networks for Demosaicing

The neural networks applied to demosaicing can mainly be subdivided into two types of macro-architectures: U-Net [11, 23, 24, 31, 37, 38] and Isotropic (often called residual-in-residual)[5, 12, 15, 28, 30, 36].

In general, the main difference between U-Net and isotropic macro-architectures lies in downsampling. U-Net networks employ progressive downsampling to capture multiple feature-scales [21], while the trunks of isotropic networks employ a uniform spatial size [28, 30, 35], and employ spatial downsampling or upsampling only at the beginning or end of the network.

For most general image restoration tasks, such as image denoising or super-resolution, an isotropic network employs no downsampling at all [13, 35]. For demosaicing, while many isotropic networks also do not perform down-

Name	Year	Downsampling Ratio	GFLOPs
DeepJoint[5]	2016	2	14
MMNet[10]	2018	1	18
RNAN [36]	2019	1	162
TENet [20]	2019	2	3199
SGNet [15]	2020	2	-
JDNDM[30]	2021	2	408
GRL[12]	2023	1	491
ESUM[28]	2025	1	408

Table 1. Previous Isotropic Networks Applied to Demosaicing. FLOPs calculated for 256x256 image. SGNet does not have fully available code, so FLOPs cannot be calculated. Previous isotropic demosaicing networks do not use downsampling greater than two.

sampling [12, 28, 36], some networks perform "packing", which folds a CFA pattern into a single pixel[5, 30]. However, prior networks do not explicitly use downsampling to improve efficiency and do not exceed 2x downsampling. A brief summary of prior isotropic networks for demosaicing is shown in Tab. 1.

Because isotropic networks tend to operate on high spatial resolutions, without employing spatial downsampling, they are often quite slow and inefficient[2]. This is a notable problem for demosaicing, since its main application field is mobile phones, which are famously compute constrained. In particular, isotropic networks for JDD can be several hundred G-FLOPs for 256-by-256 pixel images[28, 30], which are several orders of magnitude larger than networks typically designed for image recognition on mobile devices[6, 22].

In this paper, we argue that a crucial step in improving the efficiency of an isotropic JDD network is deliberately employing spatial downsampling for the express purpose of improving efficiency, at a factor greater than previously explored.

### 2.3. Zero-Shot Neural Architecture Search

The primary tool we will use to make this argument is Zero-Shot Neural Architecture Search (NAS). In contrast to conventional NAS techniques, Zero-Shot NAS attempts to find a performant neural network architecture without any training, often based on mathematical observations regarding the nature of deep neural networks[14, 25, 26]. This is attractive for designing networks in a principled manner, and is the primary reason we employ Zero-Shot NAS techniques in this paper.

Often, Zero-Shot NAS techniques employ the Principle of Maximum Entropy, which aims to maximize the entropy of the feature map outputted by the network [14, 25]. In particular, this paper focuses on the DeepMAD[25] entropy formulation, which is designed for convolutional neural net-

works and takes the following form:

$$H_L \triangleq \log(r_{L+1}^2 c_{L+1}) \sum_{i=1}^L \log(c_i k_i^2 / g_i). \quad (1)$$

In the above equation,  $H_L$  is the entropy,  $r_{L+1}$  is the final resolution (before global average pooling),  $c_{L+1}$  is the final number of channels,  $c_i$ ,  $k_i$  and  $g_i$  are the input channel, kernel size, and number of convolutional groups to the  $i$ -th layer respectively.

To use this entropy score to find performant CNNs, DeepMAD constrains the ratio of width to depth  $\rho = L/w$ , as well as the desired FLOPs and parameters, and then finds the CNN with maximum entropy under the constraints. Thus, DeepMAD compresses a complex search with many parameters into a simple search across a single parameter  $\rho$ , which can be done via mathematical programming. We will employ a modified version of this technique to compare downsampled and non-downsampled isotropic networks.

## 3. Methods

### 3.1. Network Design

Our primary goal in this paper is to compare downsampled and non-downsampled isotropic networks. To do this, we make the following design choices:

1. First, we design JD3Net as a simple fully convolutional network, forgoing any complex attention mechanisms that can be often found in image restoration. By using highly simple networks, we can be more confident that results are attributable to macro-architecture design.
2. Second, we employ mathematical architecture design to choose our specific network parameters, such as width or downsampling ratio. Using mathematical architecture design allows us to design representative architectures for downsampled and non-downsampled variants of JD3Net in a principled manner, without searching across the entire space of potential JD3Net networks.

JD3Net employs modified variants of NAFBlocks[1], with the attention removed, and which we will refer to as Simplified-NAFBlocks. A specific illustration of NAFBlocks and Simplified-NAFBlocks can be found in Fig. 3.

Our decision to remove channel attention from JD3Net is due to the implementation complexity of attention in image restoration networks. For instance, techniques such as Test-time Local Converter[3] are used by some networks, but not others. Moreover, we provide some brief ablation in Sec. 4.5, which shows that the Simple Channel Attention (SCA) mechanism used by NAFNet actually decreases the performance of JD3Net. Since JD3Net can achieve strong empirical performance without complex attention mechanisms, we leave the investigation of attention for downsampled isotropic networks to future work.

In terms of the overall architecture of JD3Net, we employ a typical isotropic design. Where  $d$  is the down-sampling ratio and  $B$  is the number of blocks, our networks consist of a  $d \times d$  convolutional layer to begin, then  $B$  Simplified-NAFBlocks, and finally a  $1 \times 1$  convolution and a  $d \times d$  PixShuffle layer to return our image to the original resolution (see Fig. 3).

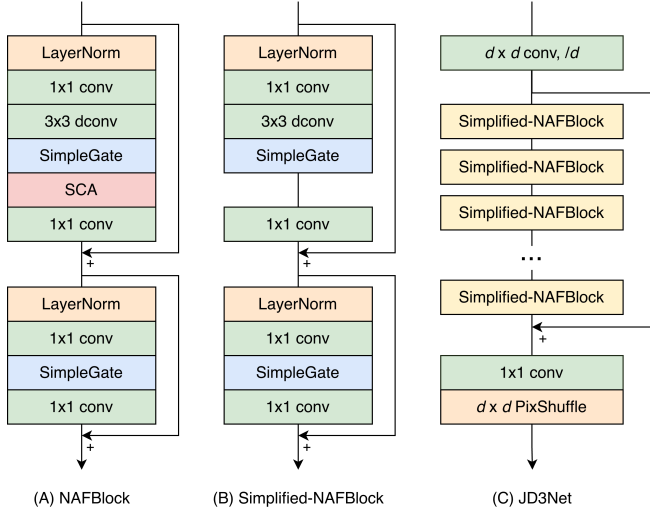


Figure 3. Simplified-NAFBlock and JD3Net Architecture. (A) NAFBlock. SCA stands for Simple Channel Attention. Dconv stands for depthwise convolution. (B) Simplified-NAFBlock, which is the same as NAFBlock except for removal of SCA. (C) Our fully-convolutional JD3Net architecture. JD3Net is fully-convolutional and highly simple.

We detail our selection of depth, width, and downsampling ratio with mathematical architecture design in the following section.

### 3.2. Mathematical Architecture Design

As previously stated, we modify DeepMAD’s entropy score to design JD3Net. The principal issue with applying DeepMAD directly to image restoration is that its entropy score is reliant on the spatial resolution of the input image (ie a network would have a different entropy score with a  $256 \times 256$  image compared to a  $512 \times 512$  image). Consequently, DeepMAD selects different networks depending on the input resolution. For classification, where input resolution is an active consideration in network design [16, 27], this makes sense. But for image restoration, where networks should be able to process an arbitrary image, we would prefer our selection of network to be invariant to the input resolution.

To achieve a resolution-invariant entropy score, instead of summing across the size of the entire final feature map, we utilize the channel density (number of channels per output pixel). Our modified entropy score is thus as such:

$$H_L \triangleq \log(c_{L+1}/d^2) \sum_{i=1}^L \log(c_i k_i^2 / g_i). \quad (2)$$

Similar to DeepMAD, we perform a search across the ratio of width and depth  $\rho$ . However, noting the heuristical nature of entropy scores, we also find that our entropy score over-promotes downsampling, with downsampling ratios of 6 or 8 in larger networks. However, since a strong local modeling capability is still crucial to the success of isotropic networks, we find more success constraining the downsampling ratio to 4. Additionally, unlike DeepMAD, since our primary concern is FLOPs efficiency, we do not apply a parameter constraint. Finally, since the number of blocks is linearly related with the number of convolutions, for notational simplicity, we constrain  $\rho = B/w$ , where  $B$  is the number of blocks.

Thus, our approach takes the following mathematical programming formulation:

$$\begin{aligned} \max_{w,d,B} \quad & H_L \\ \text{s.t.} \quad & B/w \leq \rho \\ & d \leq 4 \\ & \text{FLOPs} \leq \text{budget} \end{aligned} \quad (3)$$

Solving this mathematical programming problem will result in the entropy-maximizing values for  $B$ ,  $w$ , and  $d$ , under the constraint of  $\rho$ . In Sec. 4.1, we will show that the optimal downsampling ratio  $d$  is greater than one for most practical choices of network, and perform our search to find an effective network.

## 4. Experiments and Analysis

### 4.1. Searching for JD3Net

As noted previously, we design two networks, one smaller and one larger. JD3Net was constrained to 128 GFLOPs for a  $256 \times 256$  image, which is more comparable to existing image restoration and JDD networks, while JD3Net-S was constrained to only 25 GFLOPs for a  $256 \times 256$  image, which is more suitable for mobile applications. For simplicity, we let  $w$  and  $B$  be multiples of 4.

We perform our search for JD3Net by comparing validation PSNRs on the Hard Demosaicing Dataset[28], a dataset of 638 real world joint-demosaicing-and-denoising images from 17 difficult scenes. Specifically, we compare results on the most noisy setting, ISO 3200. We train for 150 epochs using the provided pre-processed  $48 \times 48$  hard training patches. Learning rate is 0.001 on Adam optimizer with MSE loss (following ESUM[28]). Batch size for the smaller network is 64, and 48 for the larger network.

For JD3Net-S, we find that  $\rho = 1.0$  is optimal, resulting in  $(d, w, B) = (3, 64, 64)$ , while for base JD3Net,  $\rho = 1.2$

is optimal, resulting in  $(d, w, B) = (4, 128, 152)$ . Thus, our search results reveal that  $d > 1$  maximizes entropy for most practical isotropic networks.

Additionally, we perform a similar search for networks without downsampling. We refer to the small and normal variants as JD3Net-S-x1 and JD3Net-x1. All search results can be found in Tab. 2

To compare these networks, we assess on the test set of the ISO3200 split of the HDD dataset, shown in Tab. 3. As expected, JD3Net and JD3Net-S with downsampling outperform their counterparts without downsampling. JD3Net-S, the smaller network of the two, in particular experiences a large improvement in performance with downsampling, with a 0.29 PSNR increase on average. Overall, these results indicate the efficacy of downsampling in designing efficient isotropic demosaicing networks.

Network	GFLOPs Constraint	$\rho$	$d$	$w$	$B$	Val. PSNR
JD3Net-S	25	0.5	4	96	48	44.146
		0.7	4	88	60	44.132
		<b>1.0</b>	<b>3</b>	<b>64</b>	<b>64</b>	<b>44.148</b>
		1.2	3	60	72	44.146
		1.5	3	56	84	44.136
JD3Net-S-x1	25	0.5	1	40	16	44.02
		<b>0.7</b>	<b>1</b>	<b>36</b>	<b>20</b>	<b>44.03</b>
		1.0	1	28	28	43.99
		1.2	1	28	32	44.02
		1.5	1	24	36	43.89
JD3Net	128	0.5	4	172	84	44.136
		0.7	4	152	104	44.286
		1.0	4	136	132	44.272
		<b>1.2</b>	<b>4</b>	<b>128</b>	<b>152</b>	<b>44.294</b>
		1.5	4	120	172	44.284
JD3Net-x1	128	0.5	1	68	32	44.209
		0.7	1	60	40	44.216
		1.0	1	52	52	44.242
		1.2	1	48	56	44.232
		<b>1.5</b>	<b>1</b>	<b>48</b>	<b>64</b>	<b>44.244</b>

Table 2. Search Results for JD3Net and non-downsampled JD3Net. FLOPs on a 256x256 pixel image.

Network	Single	Quad	Nona
JD3Net-S-x1	48.83	48.37	47.86
<b>JD3Net-S</b>	<b>49.06</b>	<b>48.61</b>	<b>48.26</b>
JD3Net-x1	49.27	48.85	48.43
<b>JD3Net</b>	<b>49.36</b>	<b>48.99</b>	<b>48.54</b>

Table 3. Comparison of Downsampled and non-Downsampled JD3Nets on HDD ISO3200. Metric is Test PSNR.



Figure 4. Qualitative Results for ESUM and JD3Net on HDD. All are ISO 3200 Nona Bayer. Demosaicing occurred on RAW images, but post-processing was done with a normal ISP pipeline to make the images visually normal. JD3Net produces more detailed and accurate images with less computational cost.

## 4.2. Real Image Unified Joint-Demosaicing-and-Denoising

To evaluate the performance of JD3Net and JD3Net-S comprehensively, we evaluate both JD3Net and JD3Net-S on all 4 difficulty settings of the Hard Demosaicing Dataset. Training settings are identical to those in Sec. 4.1. In order to allow JD3Net to take multiple CFA patterns as input, we use ESUM’s technique of appending CFAs to the input images.

Averaged across all CFA patterns and all noise levels, JD3Net-S achieves only 0.1 PSNR less than ESUM[28] while being 16.3 times faster, while JD3Net outperforms ESUM by 0.35 PSNR while being 3.2 times faster. We show a selection of qualitative results between JD3Net and ESUM in Fig. 4, which demonstrates the better reconstruction capability of JD3Net. Quantitative results are given in Tab. 4.

## 4.3. Synthetic Quad-Bayer HybridEVS Demosaicing

We also evaluate JD3Net on synthetic quad-bayer HybridEVS demosaicing. We train on the MIPI dataset [29] training split for  $8 \cdot 10^6$  iterations at a batch size of 20. We use PSNR loss[1] and Adam optimizer with a learning rate of 0.001. We apply the data augmentations used

Network	GFLOPs	ISO 400			ISO 800			ISO 1600			ISO 3200			Avg
		Single	Quad	Nona										
JDNDM[30]	408	53.69	-	-	<b>52.34</b>	-	-	50.43	-	-	49.00	-	-	-
BJDD[23]	69	-	50.86	-	-	50.05	-	-	48.88	-	-	47.50	-	-
SAGAN[24]	342	-	-	49.55	-	-	49.06	-	-	48.05	-	-	46.88	-
KLAP[11]	106	53.27	52.01	50.44	51.91	50.99	49.79	50.28	49.40	48.59	48.95	48.10	47.20	50.08
ESUM[28]	408	<b>53.75</b>	<b>52.68</b>	<b>51.96</b>	52.17	<b>51.36</b>	50.76	<b>50.64</b>	<b>50.01</b>	49.46	48.98	48.57	48.11	<b>50.70</b>
JD3Net-S	25	53.42	52.34	50.92	52.21	51.35	<b>50.92</b>	50.56	49.95	<b>49.56</b>	<b>49.06</b>	<b>48.61</b>	<b>48.26</b>	50.60
JD3Net	128	<b>54.06</b>	<b>53.16</b>	<b>52.38</b>	<b>52.64</b>	<b>51.95</b>	<b>51.29</b>	<b>50.92</b>	<b>49.42</b>	<b>49.86</b>	<b>49.36</b>	<b>48.99</b>	<b>48.54</b>	<b>51.05</b>

Table 4. HDD Results (PSNR). Bold is best. Blue is second-best. FLOPs on 256x256 pixel image. Average PSNR is calculated for unified models.

Network	GFLOPs	Kodak	McMaster	BSD100	Urban100	WED	Avg
BMTNet*[38]	7	37.69/0.980	34.79/0.950	36.11/0.981	34.45/0.973	33.95/0.965	35.398/0.970
NAFNet[1](w-32)	32	38.60/0.980	36.18/0.961	37.12/0.985	35.63/0.978	<b>35.24/0.972</b>	36.554/0.975
TSANet-S[37]	37	38.73/0.984	-	36.56/0.984	<b>36.15/0.980</b>	<b>35.19/0.973</b>	<b>36.658/0.980</b>
JD3Net-S (Ours)	25	<b>38.93/0.990</b>	<b>36.57/0.985</b>	<b>37.18/0.987</b>	<b>35.90/0.985</b>	<b>35.09/0.983</b>	<b>36.734/0.986</b>
Restormer[32]	282	39.16/0.986	36.54/0.967	37.11/0.985	36.36/0.977	35.00/0.971	36.83/0.977
SAGAN[24]	342	36.14/0.959	32.58/0.939	30.53/0.931	29.89/0.946	28.22/0.917	31.47/0.938
TSANet-L[37]	149	<b>39.40/0.986</b>	-	37.34/0.986	37.07/0.983	<b>35.76/0.977</b>	37.393/0.983
DemosaicFormer[31]	491	39.32/0.982	<b>37.88/0.963</b>	<b>37.65/0.982</b>	<b>37.64/0.980</b>	<b>34.86/0.986</b>	<b>37.47/0.979</b>
JD3Net (Ours)	128	<b>39.63/0.991</b>	<b>37.40/0.987</b>	<b>37.85/0.989</b>	<b>37.18/0.987</b>	<b>36.18/0.987</b>	<b>37.64/0.988</b>

Table 5. Synthetic Quad-Bayer HybridEVS Demosaicing Results (PSNR/SSIM). Top are smaller networks, bottom are larger networks. Bold is best (PSNR or SSIM) within its section. Blue is second best. As before, FLOPs calculated on 256x256 image. As TSANet code has not been released, we could not benchmark it on McMaster. For a similar reason, average PSNR/SSIM for TSANet does not include McMaster. \*Binarized networks.

by DemosaicFormer[31] in the first part of their schedule, which is to synthetically generate rotated and flipped HybridEVS mosaics from MIPI’s ground truth images. Following BMTNet[38], we evaluate on synthetically generated quad-bayer HybridEVS mosaics, which are generated from the Kodak[17], McMaster[34], BSD100[19] and Urban100[8] datasets, as well as the first hundred images of the Waterloo Exploration Database (WED)[18]. CFA appending is utilized for both JD3Net-S and JD3Net.

Against DemosaicFormer[31], the previous state-of-the-art method, JD3Net achieves comparable performance with 3.8 times fewer FLOPs, scoring better overall on Kodak, BSD100, and WED, and scoring better SSIM on McMaster and Urban100. Averaged across all 5 datasets, JD3Net improves by 0.17 PSNR compared to DemosaicFormer while being 3.8 times faster. JD3Net-S outperforms TSANet-S by 0.08 PSNR while being 48% faster. Quantitative results

are shown in Tab. 5. Some qualitative results of DemosaicFormer and JD3Net are shown in Fig. 5, which demonstrates the improved reconstruction capability of JD3Net, in particular in reconstructing the original color.

#### 4.4. Synthetic Bayer Demosaicing

We also evaluate JD3Net on synthetic bayer demosaicing with the Kodak[17] and McMaster[34] datasets. Following GRL[12], we train both networks on the ImageNet train split. JD3Net is trained on 128x128 patches at a batch size of 20, while JD3Net-S is trained on 129x129 patches (for divisibility by 3) at a batch size of 32, both for  $10^6$  iterations. As before, we use PSNR loss and Adam optimizer with a learning rate of 0.001, with random flipping and rotation augmentations. CFA appending is used for JD3Net-S, but since a 4x downsampling can learn the CFA pattern inherently, CFA appending is not necessary for JD3Net.

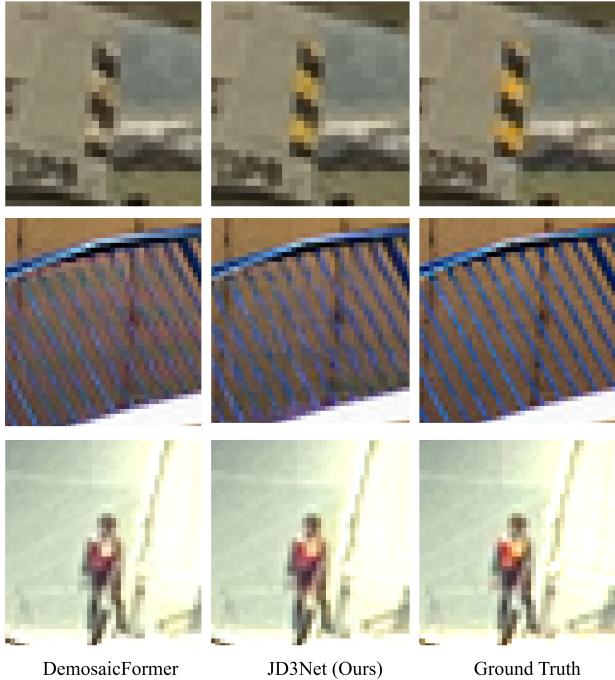


Figure 5. Qualitative Results for DemosaicFormer and JD3Net on Quad-Bayer HybridEVS demosaicing.

Network	GFLOPs	Kodak	McMaster
DeepJoint[5]	14	42.00	39.14
RNAN[36]	162	43.16	39.70
DRUNet[33]	278	42.68	39.39
GRL-S[12]	491	<b>43.57</b>	<b>40.22</b>
JD3Net-S	25	42.27	39.44
JD3Net	128	<b>43.65</b>	<b>40.07</b>

Table 6. Kodak and McMaster Results (PSNR). Bold is best. Blue is second best. As before, FLOPs calculated on 256x256 image.

JD3Net achieves competitive performance with GRL-S while using 3.8 times fewer FLOPs, exceeding GRL-S’s performance on Kodak but falling behind on McMaster. Additionally, JD3Net’s architecture is notably much simpler than GRL, with JD3Net being fully convolutional and GRL employing complex attention mechanisms.

#### 4.5. Ablation

For the most part, ablation of JD3Net is performed implicitly through the process of its design. For instance, the effects of different depth/width ratios or downsampling can be found in Sec. 4.1. Moreover, JD3Net is an extremely simple network; consequently, there are not many components to ablate on. Nonetheless, since we modify NAFNet’s[1]

Network	Single	Quad	Nona
JD3Net-S	49.06	48.61	48.26
JD3Net-S + SCA	49.10	48.65	48.30
JD3Net	49.36	48.99	48.54
JD3Net + SCA	48.95	48.54	48.06

Table 7. Ablation testing for channel attention in JD3Net. SCA is simple channel attention. Results are test PSNR for ISO3200 HDD. Channel attention improves JD3Net-S but causes JD3Net to overfit.

NAFBlock by removing attention, here we offer some brief ablations on the effect of attention on our networks, using the ISO3200 split of HDD.

Attention ablation results can be found in Tab. 7. As expected, including NAFNet’s Simple Channel Attention (SCA) improves the performance of JD3Net-S, but unexpectedly, it causes JD3Net to overfit and decreases performance. This can potentially be attributed to the relatively small size of real-image JDD datasets, and thus the fragility of network architectures trained upon them. Nonetheless, as the effects of attention are outside the topic of investigation of this paper, and JD3Net performs strongly without attention, we leave the design of attention for downsampled isotropic networks for future work.

## 5. Conclusion

This paper has shown the effectiveness of downsampling in isotropic networks for JDD and image demosaicing on a variety of datasets. JD3Net significantly exceeds both state-of-the-art performance and efficiency for JDD on the Hard Demosaicing Dataset. For Bayer Demosaicing and Quad-Bayer HybridEVS Demosaicing, JD3Net achieves competitive performance and state-of-the-art efficiency. Notably, JD3Net is a simple fully convolutional network, while many of the methods we compared against in this paper, such as GRL or DemosaicFormer, employ substantially more complex and custom-tuned mechanisms, such as custom attention or state-space modules. Finally, while the focus of this paper was isotropic networks, similarly JD3Net outperformed many strong U-Net architectures. Overall, JD3Net is a simple demonstration of the effectiveness of downsampling for JDD, and we expect that future isotropic networks can leverage both spatial downsampling and special JDD/demosaicing-specific network design to achieve even greater performance.

## References

- [1] Liangyu Chen, Xiaojie Chu, Xiangyu Zhang, and Jian Sun. Simple baselines for image restoration. 2022. 3, 5, 6, 7
- [2] Xin Chen, Zhiyuan Li, Yizhou Pu, Yiqi Liu, Jun Zhou, Yu

- Qiao, and Chao Dong. A comparative study of image restoration networks for general backbone network design. In *Proceedings of the IEEE/CVF Conference on Computer Vision and Pattern Recognition (CVPR)*, 2024. 2, 3
- [3] Xiaojie Chu, Liangyu Chen, Chengpeng Chen, and Xin Lu. Improving image restoration by revisiting global information aggregation. *arXiv preprint arXiv:2112.04491*, 2021. 3
- [4] Alexey Dosovitskiy, Lucas Beyer, Alexander Kolesnikov, Dirk Weissenborn, Xiaohua Zhai, Thomas Unterthiner, Mostafa Dehghani, Matthias Minderer, Georg Heigold, Sylvain Gelly, Jakob Uszkoreit, and Neil Houlsby. An image is worth 16x16 words: Transformers for image recognition at scale. In *International Conference on Learning Representations (ICLR)*, 2021. 1
- [5] Michaël Gharbi, Gaurav Chaurasia, Sylvain Paris, and Frédo Durand. Deep joint demosaicking and denoising. In *Proceedings of the 9th ACM SIGGRAPH Conference and Exhibition on Computer Graphics and Interactive Techniques in Asia*, 2016. 2, 3, 7
- [6] Andrew Howard, Mark Sandler, Grace Chu, Liang-Chieh Chen, Bo Chen, Mingxing Tan, Weijun Wang, Yukun Zhu, Ruoming Pang, Vijay Vasudevan, Quoc V. Le, and Hartwig Adam. Searching for mobilenetv3. In *Proceedings of the IEEE/CVF International Conference on Computer Vision (ICCV)*, 2019. 3
- [7] Hakki Can Karaimer and Michael S. Brown. A software platform for manipulating the camera imaging pipeline. In *European Conference on Computer Vision (ECCV)*, 2016. 1
- [8] Jun-Hyuk Kim, Jun-Ho Choi, Manri Cheon, and Jong-Seok Lee. Urban100 dataset, 2024. 6
- [9] Thomas Klatzer, Kerstin Hammernik, Patrick Knöbelreiter, and Thomas Pock. Learning joint demosaicing and denoising based on sequential energy minimization. In *Proceedings of the IEEE International Conference on Computational Photography (ICCP)*, 2016. 2
- [10] Filippos Kokkinos and Stamatios Lefkimmiatis. Iterative joint image demosaicking and denoising using a residual denoising network. In *Proceedings of the European Conference on Computer Vision (ICCV)*, 2018. 3
- [11] Hyeon Lee, Dongwoo Park, Wooseok Jeong, Kyoungho Kim, Hyunjin Je, Dooyoung Ryu, and Se Young Chun. Efficient unified demosaicing for bayer and non-bayer patterned image sensors. In *Proceedings of the IEEE/CVF International Conference on Computer Vision (ICCV)*, 2023. 2, 6
- [12] Yawei Li, Yuchen Fan, Xiaoyu Xiang, Denis Demandolx, Rakesh Ranjan, Radu Timofte, and Luc Van Gool. Efficient and explicit modelling of image hierarchies for image restoration. In *Proceedings of the IEEE Conference on Computer Vision and Pattern Recognition (CVPR)*, 2023. 2, 3, 6, 7
- [13] Jingyun Liang, Jiezhong Cao, Guolei Sun, Kai Zhang, Luc Van Gool, and Radu Timofte. Swinir: Image restoration using swin transformer. In *Proceedings of the IEEE/CVF International Conference on Computer Vision (ICCV) Workshops*, 2021. 2
- [14] Ming Lin, Peng Wang, Zhaoliang Sun, Hao Chen, Xiang Sun, Qiaolin Qian, Haoxiang Li, and Rong Jin. Zen-nas: A zero-shot nas for high-performance image recognition. In *Proceedings of the IEEE/CVF International Conference on Computer Vision (ICCV)*, 2021. 3
- [15] Lin Liu, Xi Jia, Jian Liu, and Qi Tian. Joint demosaicing and denoising with self-guidance. In *Proceedings of the IEEE/CVF Conference on Computer Vision and Pattern Recognition (CVPR)*, 2020. 1, 2, 3
- [16] Zhuang Liu, Hanzi Mao, Chao-Yuan Wu, Christoph Feichtenhofer, Trevor Darrell, and Saining Xie. A convnet for the 2020s. *Proceedings of the IEEE/CVF Conference on Computer Vision and Pattern Recognition (CVPR)*, 2022. 4
- [17] Alexander C Loui, Jiebo Luo, Shih-Fu Chang, Dan Ellis, Wei Jiang, Lyndon Kennedy, Keansub Lee, and Akira Yanagawa. Kodak’s consumer video benchmark data set: concept definition and annotation. In *Proceedings of the International Workshop on Multimedia Information Retrieval*, 2007. 6
- [18] Kede Ma, Zhengfang Duanmu, Qingbo Wu, Zhou Wang, Hongwei Yong, Hongliang Li, and Lei Zhang. Waterloo Exploration Database: New challenges for image quality assessment models. *IEEE Transactions on Image Processing*, 26(2):1004–1016, 2017. 6
- [19] D. Martin, C. Fowlkes, D. Tal, and J. Malik. A database of human segmented natural images and its application to evaluating segmentation algorithms and measuring ecological statistics. In *Proceedings of the International Conference on Computer Vision (ICCV)*, pages 416–423, 2001. 6
- [20] Guocheng Qian, Yuanhao Wang, Jinjin Gu, Chao Dong, Wolfgang Heidrich, Bernard Ghanem, and Jimmy S Ren. Rethink the pipeline of demosaicking, denoising, and super-resolution. *arXiv preprint arXiv:1905.02538*, 2019. 2, 3
- [21] Olaf Ronneberger, Philipp Fischer, and Thomas Brox. U-net: Convolutional networks for biomedical image segmentation. In *Proceedings of the International Conference on Medical Image Computing and Computer-Assisted Intervention (MICCAI)*, 2015. 2
- [22] Mark Sandler, Andrew Howard, Menglong Zhu, Andrey Zhmoginov, and Liang Chen. Mobilenetv2: Inverted residuals and linear bottlenecks. In *Proceedings of the IEEE/CVF Conference on Computer Vision and Pattern Recognition (CVPR)*, 2018. 3
- [23] SMA Sharif, Rizwan Ali Naqvi, and Mithun Biswas. Beyond joint demosaicking and denoising: An image processing pipeline for a pixel-bin image sensor. In *Proceedings of the IEEE/CVF Conference on Computer Vision and Pattern Recognition*, pages 233–242, 2021. 1, 2, 6
- [24] SMA Sharif, Rizwan Ali Naqvi, and Mithun Biswas. Sagan: Adversarial spatial-asymmetric attention for noisy non-bayer reconstruction. In *Proceedings of the British Machine Vision Conference (BMVC)*, 2021. 1, 2, 6
- [25] Xiaohong Shen, Yifan Wang, Ming Lin, Yujing Huang, Hao Tang, Xiang Sun, and Yong Wan. Deepmad: Mathematical architecture design for deep convolutional neural network. In *Proceedings of the IEEE/CVF Conference on Computer Vision and Pattern Recognition (CVPR)*, 2023. 2, 3
- [26] Zhaoliang Sun, Ming Lin, Xiang Sun, Zechun Tan, Haoxiang Li, and Rong Jin. Mae-det: Revisiting maximum entropy principle in zero-shot nas for efficient object detection.

- In *Proceedings of the International Conference on Machine Learning (ICML)*, 2022. 3
- [27] Mingxin Tang and Quoc V Le. Efficientnet: Rethinking model scaling for convolutional neural networks. 2019. 4
- [28] Samuel Tedla, Abhijith Punnappurath, Long Zhao, and Michael Brown. Examining joint demosaicing and denoising for single-, quad-, and nona-bayer patterns. In *Proceedings of the IEEE International Conference on Computational Photography (ICCP)*, 2025. 1, 2, 3, 4, 5, 6
- [29] Yaqi Wu, Zhihao Fan, Xiaofeng Chu, Jimmy S. Ren, Xiaoming Li, Zongsheng Yue, Chongyi Li, Shangcheng Zhou, Ruicheng Feng, Yuekun Dai, Peiqing Yang, Chen Change Loy, Senyan Xu, Zhijing Sun, Jiaying Zhu, Yurui Zhu, Xueyang Fu, Zheng-Jun Zha, Jun Cao, Cheng Li, Shu Chen, Liang Ma, Shiyang Zhou, Haijin Zeng, Kai Feng, Yongyong Chen, Jingyong Su, Xianyu Guan, Hongyuan Yu, Cheng Wan, Jiamin Lin, Binnan Han, Yajun Zou, Zhuoyuan Wu, Yuan Huang, Yongsheng Yu, Daoan Zhang, Jizhe Li, Xuanwu Yin, Kunlong Zuo, Yunfan Lu, Yijie Xu, Wenzong Ma, Weiyu Guo, Hui Xiong, Wei Yu, Bingchun Luo, Sabari Nathan, and Priya Kansal. Mipi 2024 challenge on demosaic for hybridevs camera: Methods and results, 2024. 5
- [30] Wei Xing and Karen Egiazarian. End-to-end learning for joint image demosaicing, denoising, and super-resolution. In *Proceedings of the IEEE/CVF Conference on Computer Vision and Pattern Recognition (CVPR)*, 2021. 1, 2, 3, 6
- [31] Senyan Xu, Zhijing Sun, Jiaying Zhu, Yurui Zhu, Xueyang Fu, and Zheng-Jun Zha. Demosaicformer: Coarse-to-fine demosaicing network for hybridevs camera. In *Proceedings of the IEEE/CVF Conference on Computer Vision and Pattern Recognition (CVPR) Workshops*, pages 1126–1135, 2024. 2, 6
- [32] Syed Waqas Zamir, Aditya Arora, Salman Khan, Munawar Hayat, Fahad Shahbaz Khan, and Ming-Hsuan Yang. Restormer: Efficient transformer for high-resolution image restoration. In *Proceedings of the IEEE/CVF Conference on Computer Vision and Pattern Recognition (CVPR)*, 2022. 6
- [33] Kai Zhang, Yawei Li, Wangmeng Zuo, Lei Zhang, Luc Van Gool, and Radu Timofte. Plug-and-play image restoration with deep denoiser prior. *IEEE Transactions on Pattern Analysis and Machine Intelligence*, 44(10):6360–6376, 2021. 7
- [34] Lei Zhang, Xiaolin Wu, Antoni Buades, and Xin Li. Color demosaicking by local directional interpolation and non-local adaptive thresholding. *Journal of Electronic Imaging*, 20(2):023016, 2011. 6
- [35] Yulun Zhang, Kun Li, Kai Li, Lichen Wang, Bineng Zhong, and Yan Fu. Image super-resolution using very deep residual channel attention networks. In *Proceedings of the International Conference on Computer Vision (ICCV)*, 2018. 2
- [36] Yulun Zhang, Kunpeng Li, Kai Li, Bineng Zhong, and Yun Fu. Residual non-local attention networks for image restoration. In *Proceedings of the International Conference on Learning Representations (ICLR)*, 2019. 2, 3, 7
- [37] Shiyang Zhou, Haijin Zeng, Yunfan Lu, Yongyong Chen, Jie Liu, and Jingyong Su. Lightweight quad bayer hybridevs demosaicing via state space augmented cross-attention. *arXiv preprint arXiv:2309.05239*, 2025. 2, 6
- [38] Shiyang Zhou, Haijin Zeng, Yunfan Lu, Tong Shao, Ke Tang, Yongyong Chen, Jie Liu, and Jingyong Su. Binarized mamba-transformer for lightweight quad bayer hybridevs demosaicing. In *Proceedings of the IEEE/CVF Conference on Computer Vision and Pattern Recognition*, 2025. 1, 2, 6